

Yasin Yilmaz\* and Savas Evran

# Free vibration analysis of axially layered functionally graded short beams using experimental and finite element methods

**Abstract:** Free vibration behavior of short beams made of axially layered functionally graded material (FGM) was investigated experimentally and numerically. Beams, which have gradation of the material properties in the axial direction, are fabricated by powder metallurgy technique using different weight fractions of aluminum and silicon carbide powders. In order to determine elasticity modulus of axially layered functionally graded (FG) beams, homogeneous beams containing different weight fractions of Al (aluminum) and SiC (silicon carbide) are produced, and these homogeneous beams are subjected to tensile tests. Density of each homogeneous layer is also calculated experimentally. After determination of the mechanical properties of each layer of the FG beams, they are modeled in a finite element program (ANSYS) according to Timoshenko beam theory, and free vibration analyses are performed. Fundamental frequencies of the axially layered FG beams produced are also calculated experimentally. FG beams with clamped-free boundary conditions are considered. Layers of the axially FG beams are considered to have symmetric configurations. Effect of the change in weight fractions of SiC particles and sorting order of layers to fundamental frequency of the beam is investigated. Experimental results obtained are compared with numerical results.

**Keywords:** free vibration; functionally graded materials; powder metallurgy; short beam.

DOI 10.1515/secm-2014-0161

Received May 24, 2014; accepted October 12, 2014; previously published online January 20, 2015

\*Corresponding author: Yasin Yilmaz, Department of Mechanical Engineering, Pamukkale University, 20070 Denizli, Turkey, e-mail: yyilmaz@pau.edu.tr

Savas Evran: Vocational School of Technical Sciences, Canakkale Onsekiz Mart University, 17100 Canakkale, Turkey

## 1 Introduction

In 1984 functionally graded materials (FGMs) were suggested by scientists working in the field of materials science to use in high temperature environments as preparing thermal barrier materials in Japan [1]. Since then, this concept has continued to be used in different fields such as with biomedical applications [2], thermal, wear and corrosion barriers coating [3], sensor and energy applications [4], gas turbine applications [5], cutting tools [6], rotating blades [7] etc. In later years, the concept was carried out to wider areas, such as modeling and analysis of beams, shells, and plates [8, 9].

In the literature, there are many studies of free vibration analysis of beams made of FGMs, but most are limited to the case in which mechanical properties change in the thickness direction. Kapuira et al. [10] determined the static deflection and free vibration response of multi-layered FGM beams using a finite element based zigzag beam theory and supported the theoretical study with experimental work. They assumed material properties to be changed in thickness direction and used two types of FGM systems. They fabricated Al/SiC FG beam samples with three and five layers using powder metallurgy and five-layered Ni/Al<sub>2</sub>O<sub>3</sub> beam samples using combustion powder thermal spray process. Wattanasakulpong et al. [11] investigated the vibration response of FG beams layered in the thickness direction, made of alumina/epoxy produced by a multistep sequential infiltration technique. In a theoretical work, Huang and Li [12] studied free vibration behavior of axially FG Euler-Bernoulli beams with a nonuniform cross section using the integral equation method for various end supports. Pradhan and Chakraverty [13] investigated free vibration behavior of Euler and Timoshenko FG beams using classical and first-order shear deformation beam theories, assuming material properties vary continuously in the thickness direction according to the power-law exponent form. Aydogdu and Taskin [14] studied free vibration analysis of the simply supported FG beam of

variable Young modulus in the thickness direction using classical, parabolic, and exponential shear deformation beam theories. Huang et al. [15] examined free vibration behavior of homogeneous and axially FG Timoshenko beams with varying cross sections, introducing an auxiliary function in the solution process. Hein and Feklistova [16] investigated free vibration behavior of axially FG and nonuniform beams using Euler-Bernoulli beam theory and Haar wavelets. Simsek [17] carried out fundamental frequency analysis of FG beams whose material properties vary continuously through the thickness direction, using classical, first-order and different higher-order shear deformation beam theories. Sina et al. [18] analyzed free vibration behavior of FG beams, whose material properties vary through the thickness direction, using an analytical method. Su et al. [19] developed a dynamic stiffness method to investigate the free vibration behavior of functionally graded beams. They assumed material properties to vary continuously in the beam thickness direction according to a power law distribution.

As can be seen from the literature review given, there are a few theoretical studies but no experimental study on free vibration behavior of axially layered FG beams produced by powder metallurgy technique using Al/SiC powders according to research stated in open literature. In this study, free vibration behavior of axially layered short FG beams is investigated experimentally and numerically. At first, homogeneous beams that have different SiC weight fractions are produced to determine the mechanical properties of each layer that will be used in modeling axially layered FG beams in finite element analysis. These beams are also produced using powder metallurgy technique. Fundamental frequencies of these beams are calculated numerically and experimentally. The results are tabulated and compared to each other.

## 2 Materials and methods

In the literature, several techniques have been performed to produce FGMs, such as powder metallurgy [20], centrifugal casting [21], tape casting [22], laser cladding [23], plasma spray [24], chemical vapor infiltration [25], low-pressure chemical vapor deposition (LPCVD) [26], directed vapor deposition (DVD) [27], self-propagating high-temperature synthesis (SHS) [28], spark plasma sintering [29], electrophoretic deposition [30], electromagnetic separation [31], and thixotropic casting [32]. In the present study, the powder metallurgy technique is used.

### 2.1 Production of homogeneous and axially layered FG beams

Powder metallurgy technique is used in the manufacturing process of beams. Preparation of powders is important in the technique. The as-mixed powders are weighed precisely. Beams are composed of different weight fractions of aluminum (Al) and silicon carbide (SiC) powders. Zinc stearate is used as lubricant. Table 1 shows mechanical properties of Al and SiC powders obtained from the supplier. Al powders are manufactured using gas atomization technique and they have spherical structure. SiC powders are in lamellar structure. Zinc stearate is like white powder and generally used in dies as a lubricant.

In the first step, single layered homogeneous beam samples composed of specified amounts of Al and SiC powders are produced to determine mechanical properties of each layer of axially FG beams. These properties are used in numerical analysis. Totally nine homogeneous beam samples are produced by increasing the weight fraction of SiC powders from 0% to 40% with 5% increase at each step. After that, six types of five layered axially FG beams are fabricated by placing powders, obtained for different mixing ratios, in a die in a predefined sequence. Each of these axially layered FG beams has different configuration, and they are shown in Table 2. The zinc stearate is up to 2% of the total beam weight.

#### 2.1.1 Mixing of powders

Homogeneous mixing of the powders affects strength properties and sintering behaviors of the end product. Homogeneous distribution of the powders depends on physical properties of the powder, mixing method of the mixing machine, powder volume in the mixer, mixing time and speed. In the present study, powders are mixed by a Planetary Ball Miller (MTI Corporation, Richmond, USA) for 3 h reversing the rotation direction every half hour. The 12 mm balls inside each container are highly effective in

**Table 1** Mechanical properties of aluminum (Al) and silicon carbide (SiC) powders.

Properties	Aluminum (Al)	Silicon carbide (SiC)
Formula	13Al <sup>26.98</sup>	SiC <sup>40.10</sup>
Purity	99.8%	99.9%
Particle size	-100 Mesh	<1500 Grit
Melting point	660.1°C	>2000°C
Density	2.699 G/cm <sup>3</sup>	3.217 G/cm <sup>3</sup>
Mohs hardness (20°C)	2–2.9	9.2

**Table 2** %Al weight fractions of homogeneous and axially layered FG beams.

Beam type number	%Al weight fractions				
	Layer 1	Layer 2	Layer 3	Layer 4	Layer 5
Type 1	100%Al (homogeneous beam)				
Type 2	95%Al-5%SiC (homogeneous beam)				
Type 3	90%Al-10%SiC (homogeneous beam)				
Type 4	85%Al-15%SiC (homogeneous beam)				
Type 5	95	90	85	90	95
Type 6	90	95	85	95	90
Type 7	85	90	95	90	85
Type 8	90	85	95	85	90
Type 9	95	85	90	85	95
Type 10	85	95	90	95	85

homogeneous mixing of the powders. The occupancy rate of the each container volume, including balls, should not exceed three-fourths of the total volume in order to have homogeneously mixed powder. This process is also called as mechanical alloying. The Planetary Ball Miller (MTI Corporation, Richmond, USA) and contents of a container are shown in Figure 1.

### 2.1.2 Cold compacting of powders

The prepared powder mixture is cold compressed in a die under a pressure of 450 MPa using a hydraulic press. Transformation of the powder particles into the desired shape and form is achieved with compression process. A beam sample after cold pressing is shown in Figure 2.

### 2.1.3 Sintering of the beam samples

Sintering is performed on compressed beams to increase beam strength. The sintering process was carried out using an argon gas atmosphere furnace. Time-dependent



**Figure 2** A beam sample after cold pressing.

change of the furnace temperature during the sintering process is shown in Figure 3. Zinc stearate contained within the sample evaporates nearly at 335°C and is completely removed from the structure during sintering. In order to prevent oxidation of aluminum, argon gas is supplied at a constant flow rate of 50 ml/min during sintering. The final form of the beam samples are shown in Figure 4.

## 2.2 Determination of mechanical properties

Single layered homogeneous beam samples composed of specified amount of Al and SiC powders are subjected to tensile test by Instron 8801 testing device (Instron, Norwood, USA) to determine mechanical properties of each layer of axially layered FG beams. The process is realized with 0.50 mm/min speed at room temperature. In the experiments, three samples were used for each configuration, and three elastic modulus and three maximum tensile strength values obtained are averaged. In this way, elasticity modulus and maximum tensile strength of each FG beam layer are determined and given in Figures 5 and 6, respectively. As can be seen from both graphs, elastic

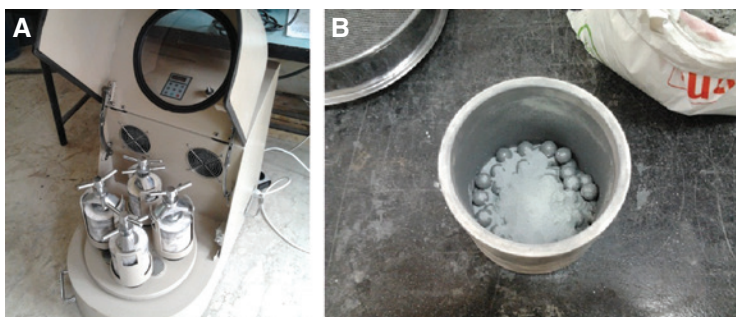


**Figure 1** (A) Planetary ball miller, (B) container.

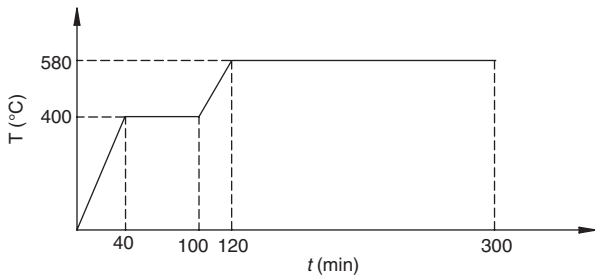


**Figure 3** Time-dependent change of furnace temperature during the sintering process.

modulus and maximum tensile strength values increase up to 15%SiC ratio and show a decreasing trend for higher percentage of SiC ratios. As far as the production technique and load carrying capacities of hydraulic press and die are concerned, it is seen that SiC weight percentage values higher than 15% are not suitable for obtaining higher elastic modulus and maximum tensile strength. Thus, the beam samples that have percentage SiC values higher than 15% are not used in the numerical part of the study.

Neelima et al. [33] investigated the mechanical behavior of Al and SiC (5%, 10%, 15%, and 20%) alloy composite materials and found that highest tensile strength can be reached for composite material composed of 15%SiC in experiments. Tensile strength values decrease for composite material composed of SiC weight percentage higher than 15%. In this study, similar results are obtained, and maximum tensile strength is observed for beams composed of 15%SiC.

### 2.3 Determination of density

Determination of density is important for free vibration analysis of axially layered FG beams in numerical analysis. In order to find density of all produced beams, weight of each beam sample was measured by a Precisa brand



**Figure 4** Axially layered FG beams.

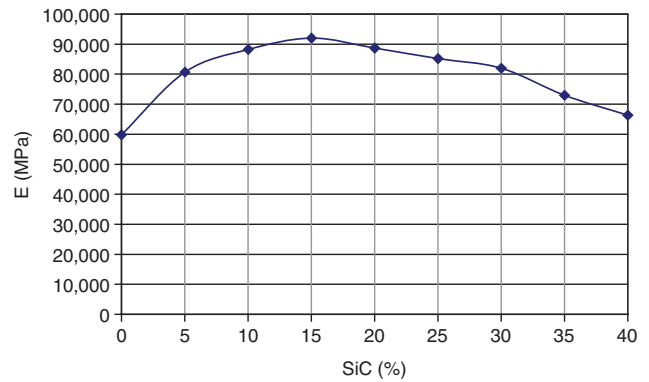


**Figure 5** Elasticity modulus values for different %SiC ratios.

sensitive balance (Precisa Gravimetrics AG, Dietikon, Switzerland). All beam samples are measured by a vernier caliper to calculate volumes of beams. After calculation of weights and volumes of beam samples, density of each beam sample are determined using density formulate ( $\rho=m/V$ ) as shown in Figure 7.

It is found that experimental density values are lower than theoretical density values. Bhattacharyya et al. [34] performed density measurements on Al/SiC FGM specimens to quantify the volume fraction of porosity in the FGM. They found that for single layer Al/SiC composite samples, the porosity increases as the ceramic content of the sample increases and the increase in porosity is more evident for multilayered composite samples. The increase in porosity is because of the fact that the ceramic reinforcements increase the viscosity of matrix, which prevents escape of air from the structure. In the present study a similar situation is also observed. Size and sharp corners of the SiC particulate also affects the porosity level of the system [35].

### 2.4 Microstructure

Microstructure characterizations of beams that have different weight percentage of SiC are monitored using

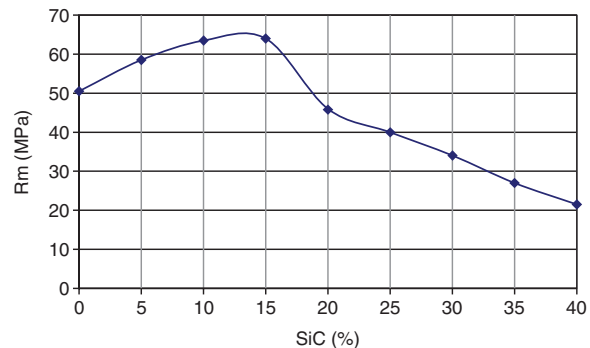


**Figure 6** Maximum tensile strength values for different %SiC ratios.

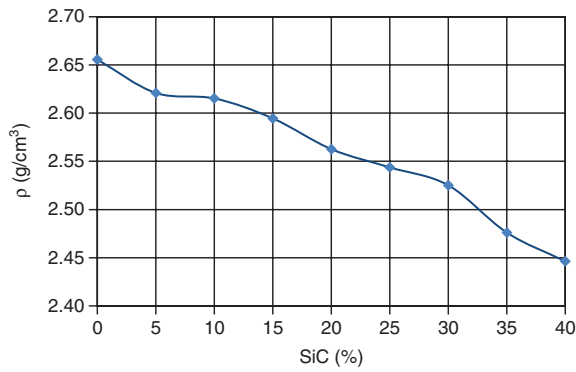


**Figure 7** Density values based on weight fractions of %SiC.

optical microscope to observe distribution of SiC alloys and presence of porosity. Size analysis of SiC particles is carried out from the micrographs (Figure 8A–D) and it is found that the typical size of SiC particles lie in the range of 2–6  $\mu\text{m}$ , which is in agreement with the expected size.

## 2.5 Free vibration analysis

Symmetric beam configurations are considered for free vibration analyses. In this way, effect of the change in weight fractions of SiC of layers to fundamental frequency of the axially layered FG beam is investigated. Beam configurations used in experimental free vibration analyses are given in Table 2 according to %Al weight fractions of the beams and layers. Type 1 to Type 4 beams are homogeneous beams each containing different weight fractions of Al and SiC particulates. Type 5 to Type 10 beams are symmetrically axially layered FG beams each have different sorting order. For experimental vibration analyses, three samples are produced from each type and average values of these three samples are used to calculate fundamental frequency of each beam configuration.

Experimental vibration measurements were performed by DEWESoft measurement instrument DEWE-43A (Dewesoft, Trbovlje, Slovenia) shown in Figure 9. It

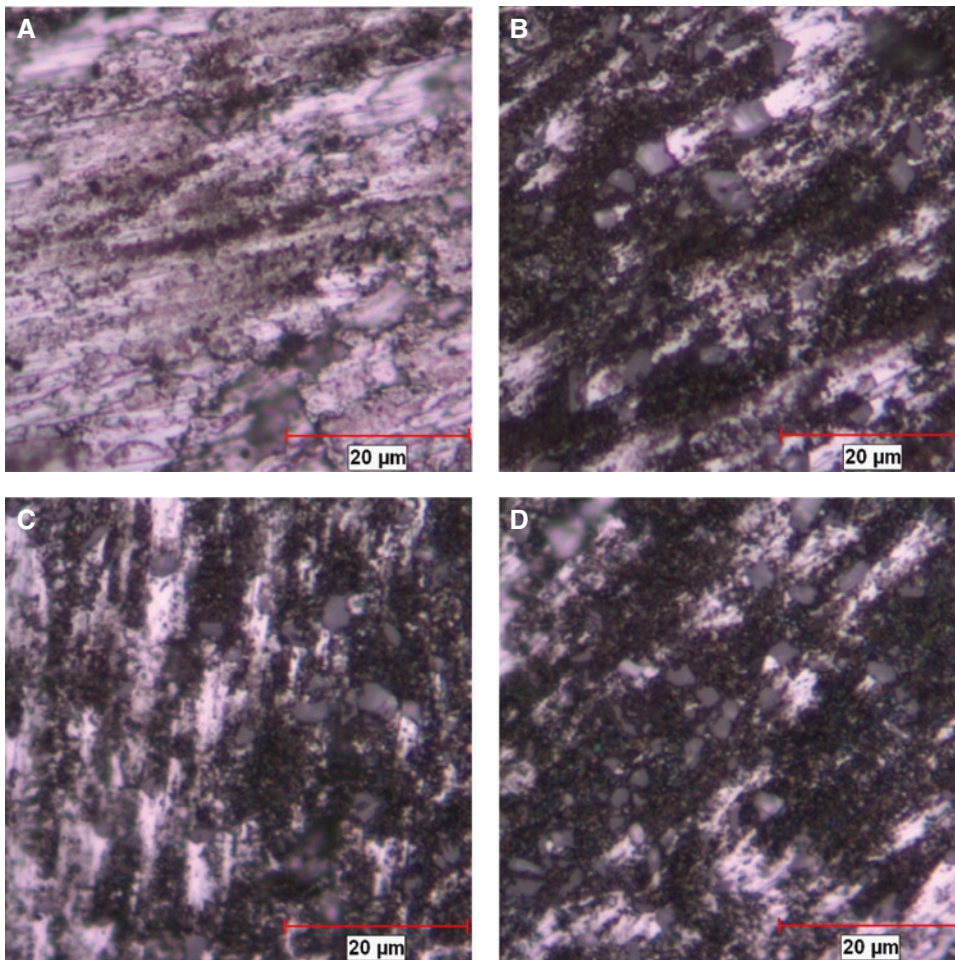


**Figure 8** Microstructure of Al/SiC beam samples (A) pure Al, (B) 5%SiC-95%Al, (C) 10%SiC-90%Al, (D) 20%SiC-80%Al.

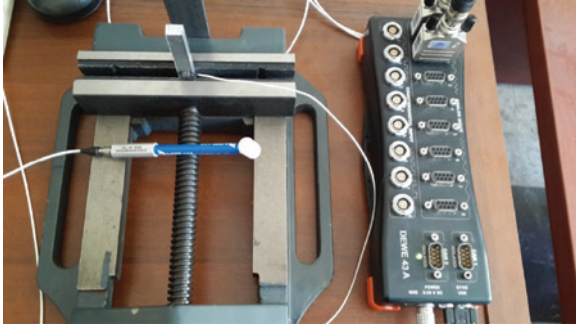


Figure 9 Modal test setup.

has eight analog inputs with 200 kS/s/ch maximum sampling rate and a 24-bit AD converter. Modal analyses are essential to predict the free vibration behavior of beams. There are many ways to carry out modal testing but impact hammer testing is mostly used. In this study, the clamped-free boundary condition was considered, each beam was fixed on one end while the other end was released to vibrate freely as shown in Figure 9. Impact hammer testing method was used to determine fundamental frequencies of the beam samples. The Dytran model 3224A1 (Dytran Instruments Inc., CA, USA) was used as an accelerometer. It is an ultra-miniature teardrop IEPE accelerometer with integral electronics and an overall weight of 0.2 g. It has a sensitivity of 10 mV/g. The Dytran model 5800SL (Dytran Instruments Inc., CA, USA) was used as an impulse hammer. It is an IEPE impulse hammer with a measurement range of 50 lbf, offering an ultra-low mass of 9.8 g and very high stiffness. It has a sensitivity of 100 mV/lbf. The reduced size and weight of the hammer head and handle reduce overall hammer inertia for quicker rebounding, which produces a very high frequency excitation, allowing the user to excite smaller structures with high-frequency content and input forcing function.

Free vibration experiments were repeated for different sorting order of layers and different weight fractions of the constituents of beams. In this way, effects of change in sorting order of the layers and change in weight fractions of SiC particles in the layers on fundamental frequency of the axially layered FG beam were determined. The results obtained were compared with ANSYS (Ansys Inc., USA) finite element program results.

### 3 Numerical analysis

Homogeneous and axially layered FG beams were modeled in finite element software (analysis system: ANSYS) using the experimentally determined elastic modulus and density values. BEAM3 element type was used in modeling.

BEAM3 is a uniaxial element with tension, compression, and bending capabilities. The element has three degrees of freedom at each node: translations in the nodal x and y directions and rotation about the nodal z-axis. Shear deformation constant is taken as 6/5 and Poisson's ratio as 0.3. Each beam has 7.7 mm thickness, 10 mm width, and 55 mm length. Fifty-five beam elements are used in the finite element model. The Block Lanczos method was used for the eigenvalue extraction. Free vibration analyses were carried out for clamped-free boundary conditions using the beam types given in Table 2, and fundamental frequency values were obtained. Schematic representation of an axially layered FG beam model is given in Figure 10.

### 4 Results and discussion

For comparison of fundamental frequencies of 10 types of beams given in Table 2 with each other, nondimensional fundamental frequencies are calculated using the

$\bar{\omega} = \omega L^2 \sqrt{\frac{\rho_{ef} A}{E_{ef} I}}$  formula [12]. Here,  $\omega$ ,  $L$ ,  $\rho_{ef}$ ,  $A$ ,  $E_{ef}$ , and  $I$  are

circular fundamental frequency, length of the beam, effective mass density, cross-sectional area, effective modulus of elasticity and cross-sectional moment of inertia, respectively. The effective material properties  $P_{ef}$  of the axially layered FG beam, such as modulus of elasticity  $E_{ef}$  and mass density  $\rho_{ef}$ , are calculated using a simple rule of mixture of composite materials as follows [36]:

$$P_{ef} = \sum_{i=1} P_i V_{f_i} \quad (1)$$

where  $P_i$  and  $V_{f_i}$  are the material properties and volume fraction of the constituent material  $i$ , and the sum of the volume fractions of all the constituent materials makes 1, i.e.,

$$\sum_{i=1} V_{f_i} = 1 \quad (2)$$

Experimental and ANSYS results are listed in Table 3. As an example, Figure 11 shows the acceleration response and its frequency spectrum for a beam of Type 5, which has a thickness of 7.60 mm. According to finite element analysis results, 85-90-95-90-85 configuration (Type 7)

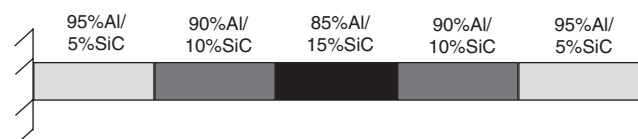


Figure 10 Schematic representation of an axially layered FG beam model.

**Table 3** Nondimensional fundamental frequencies of beams.

Beam type	Non dimensional fundamental frequencies		
	Experimental	ANSYS	% Difference
Type 1	3.0468	3.4625	12.00
Type 2	3.1287	3.4625	9.64
Type 3	3.0353	3.4625	12.34
Type 4	3.0343	3.4626	12.37
Type 5	3.0739	3.4190	10.09
Type 6	3.0438	3.4646	12.15
Type 7	3.0381	3.4923	13.00
Type 8	3.0421	3.4673	12.26
Type 9	3.0689	3.4177	10.21
Type 10	3.0371	3.4883	12.93

gives maximum nondimensional fundamental frequency, whereas experimental results show that maximum nondimensional fundamental frequency occurs for the case of 95-90-85-90-95 (Type 5) among symmetric configurations of axially layered FG beams. This result can be explained looking at the experimental fundamental frequency result of homogeneous 5%SiC-95%Al beam. Among homogeneous beams, this beam configuration gives the maximum nondimensional natural frequency. And because two layers of 5%SiC-95%Al is used in 95-90-85-90-95 configuration, the fundamental frequency of this configuration is higher than the fundamental frequency of 85-90-95-90-85 configuration.

Looking at Table 3, it is also seen that ANSYS gives higher fundamental frequencies for the configurations where a higher %SiC ratio is used at the end layers and fundamental frequency values decrease as the %SiC ratio decreases at the end layers. Whereas, according to

experimental results, fundamental frequency is maximum for the beam configurations, where 5%SiC is used at the end layers and decreases as the SiC ratio increases at the ends. Experimental results also show that sudden increase in SiC ratio between neighboring layers decreases the fundamental frequency, because a smooth transition of mechanical properties cannot be achieved for these configurations. This situation can clearly be seen from Type 5 and Type 6 beam configurations. For these configurations the effect of using a higher SiC ratio at the end layers and the effect of sudden increase in SiC ratio between neighboring layers combines, and it decreases the fundamental frequency of the beam. But for Type 7 and Type 8 configurations, these effects act in opposite directions on fundamental frequency and the effect of using a lower SiC ratio overcomes the effect of a sudden increase in SiC ratio between neighboring layers.

### 5 Conclusions

Free vibration analyses of axially layered FG beams made of Al/SiC systems using powder metallurgy technique were studied experimentally as well as numerically. The ANSYS finite element program was used for the theoretical prediction of free vibration response. Numerical and experimental results obtained are compared with each other and error rates were observed. The comparison reveals that there are some differences between experimental and theoretical results. The main cause of the differences between measured and predicted data is the fact that finite element program ANSYS does not take the porosity in the beam samples into account and assumes Al and SiC particles

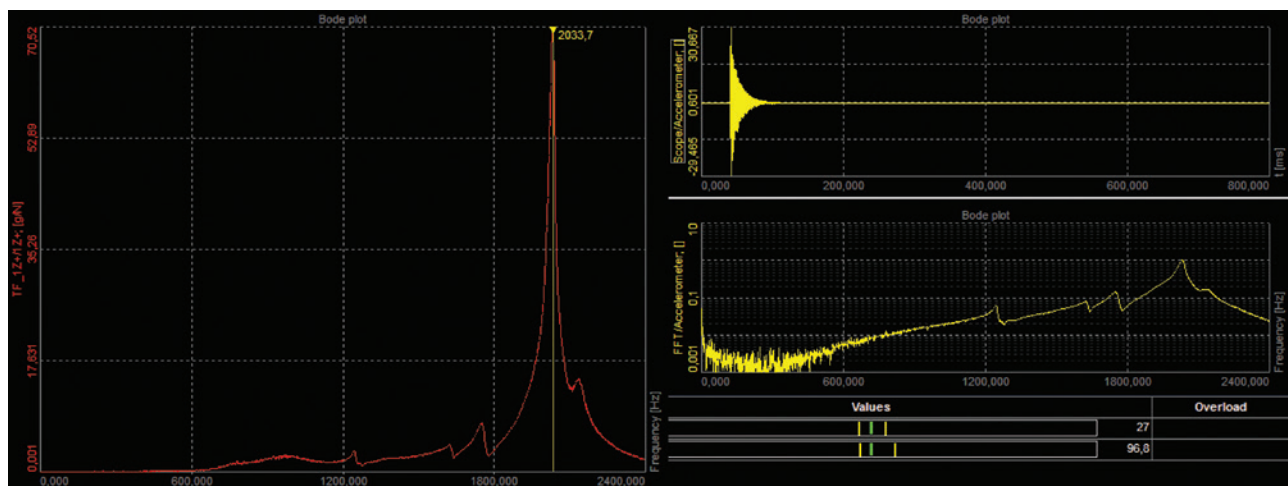


**Figure 11** Acceleration response and its frequency spectrum for a beam sample of Type 5.

to be perfectly bonded to each other. Based on the results obtained following conclusions can be drawn:

- (1) Modulus of elasticity and maximum tensile strength increase up to 15%SiC weight ratio, and after that value, they show a decreasing trend. The main causes of this behavior are the type of the system (SiC-Al) used, manufacturing technique employed, and capacity of the hydraulic press mold.
- (2) As the SiC weight ratio increases, porosity in the beam structure increases and density of the beam samples decreases.
- (3) Arrangement of axially FG beam layers has an important effect on fundamental frequency of the FG beam.
- (4) Experimental results show that sudden increase in SiC weight ratio between the neighboring layers decreases the fundamental frequency of the axially layered FG beams.

**Acknowledgments:** The authors would like to thank Pamukkale University Scientific Research Council for supporting this study under project contract no. 2013FBE007.

## References

- [1] Koizumi M. *Compos. Part B: Eng.* 1997, 28, 1–4.
- [2] Pompe W, Worch H, Epple M, Friess W, Gelinsky M, Greil P, Hempel U, Scharnweber D, Schulte K. *Mater. Sci. Eng.: A* 2003, 362, 40–60.
- [3] Schulz U, Peters M, Bach FW, Tegeder G. *Mater. Sci. Eng.: A* 2003, 362, 61–80.
- [4] Müller E, Drašar Č, Schilz J, Kaysser WA. *Mater. Sci. Eng.: A* 2003, 362, 17–39.
- [5] Leushake U, Krell T, Schulz U. *Materialwiss. Werks.* 1997, 28, 391–394.
- [6] Cho JR, Park HJ. *J. Mater. Proc. Tech.* 2002, 130–131, 351–356.
- [7] Oh SY, Librescu L, Song O. *Acta Mech.* 2003, 166, 69–87.
- [8] Carrera E, Brischetto S. *Mech. Adv. Mater. Struct.* 2010, 17, 585–585.
- [9] Carrera E, Brischetto S. *Mech. Adv. Mater. Struct.* 2011, 18, 1–2.
- [10] Kapuria S, Bhattacharyya M, Kumar AN. *Compos. Struct.* 2008, 82, 390–402.
- [11] Wattanasakulpong N, Gangadhara PB, Kelly DW, Hoffman M. *Mater. Des.* 2012, 36, 182–190.
- [12] Huang Y, Li XF. *J. Sound Vib.* 2010, 329, 2291–2303.
- [13] Pradhan KK, Chakraverty S. *Compos. Part B: Eng.* 2013, 51, 175–184.
- [14] Aydogdu M, Taskin V. *Mater. Des.* 2007, 28, 1651–1656.
- [15] Huang Y, Yang LE, Luo QZ. *Compos. Part B: Eng.* 2013, 45, 1493–1498.
- [16] Hein H, Feklistova L. *Eng. Struct.* 2011, 33, 3696–3701.
- [17] Simsek M. *Nucl. Eng. Des.* 2010, 240, 697–705.
- [18] Sina SA, Navazi HM, Haddadpour H. *Mater. Des.* 2009, 30, 741–747.
- [19] Su H, Banerjee JR, Cheung CW. *Compos. Struct.* 2013, 106, 854–862.
- [20] Kawasaki A, Watanabe R. *Ceram. Int.* 1997, 23, 73–83.
- [21] Watanabe Y, Eryu H, Matsuura K. *Acta Mater.* 2001, 49, 775–783.
- [22] Liu Z, Liu M, Nie L, Liu M. *Int. J. Hydrogen Energy* 2013, 38, 1082–1087.
- [23] Pei YT, De Hosson JTM. *Acta Mater.* 2000, 48, 2617–2624.
- [24] Gu YW, Khor KA, Fu YQ, Wang Y. *Surf. Coat. Tech.* 1997, 96, 305–312.
- [25] Kawase M, Tago T, Kurosawa M, Utsumi H, Hashimoto K. *Chem. Eng. Sci.* 1999, 54, 3327–3334.
- [26] Kim JI, Kim WJ, Choi DJ, Park JY, Ryu WS. *Carbon* 2005, 43, 1749–1757.
- [27] Groves JF, Wadley HNG. *Compos. Part B: Eng.* 1997, 28, 57–69.
- [28] Dumont AL, Bonnet JP, Chartier T, Ferreira JMF. *J. Eur. Ceram. Soc.* 2001, 21, 2353–2360.
- [29] Tang X, Zhang H, Du D, Qu D, Hu C, Xie R, Feng Y. *Int. J. Refract. Metals Hard Mater.* 2014, 42, 193–199.
- [30] Put S, Vleugels J, Van der Biest O. *J. Mater. Proc. Tech.* 2003, 143–144, 572–577.
- [31] Song CJ, Xu ZM, Li JG. *Compos. Part A: Appl. Sci. Manuf.* 2007, 38, 427–433.
- [32] Ruys AJ, Kerdic JA, Sorrell CC. *J. Mater. Sci.* 1996, 31, 4347–4355.
- [33] Neelima DC, Mahesh V, Selvaraj N. *Int. J. Appl. Eng. Res., Dindigul* 2011, 1, 793–799.
- [34] Bhattacharyya M, Kumar AN, Kapuria S. *Mater. Sci. Eng.: A*, 2008, 487, 524–535.
- [35] Nai SML, Gupta M. *Compos. Struct.* 2002, 57, 227–233.
- [36] Shen HS. *Functionally Graded Materials: Nonlinear Analysis of Plates and Shells*, CRC Press, Boca Raton, 2009.